Role of Zinc Binding in Type A Botulinum Neurotoxin Light Chain's Toxic Structure†

Li Li and Bal Ram Singh*

Department of Chemistry and Biochemistry and Center for Marine Science and Technology, University of Massachusetts Dartmouth, Dartmouth, Massachusetts 02747

Received April 3, 2000

ABSTRACT: Clostridial neurotoxins are zinc endopeptidases, and each contains one Zn^{2+}/molecule. To investigate the structural/functional role of Zn^{2+} in botulinum neurotoxin light chain (the enzymatic subunit of the neurotoxin), the effect of the removal of zinc on protein folding and enzyme kinetics was investigated. The active site Zn^{2+}, which was easily displaced from the active site by ethylenediaminetetraacetate, reversibly binds to the BoNT/A light chain (LC) in a stoichiometric manner. Enzymatic activity was completely abolished in the zinc-depleted light chain (apo-LC). However, Zn^{2+} replenishment partially restored the activity in the re-Zn^{2+}-LC (k_{cat} = 72 min^{-1}) compared to the holo-LC (k_{cat} = 140 min^{-1}). Comparable K_m values in the holo- and re-Zn^{2+}-LC were observed (41 and 55 μM, respectively), indicating a similar substrate binding ability. We investigated the structural basis of a 3-fold difference in the catalytic efficiency of the native holo-LC and re-Zn^{2+}-LC by analyzing secondary and tertiary structural parameters. Removal of the zinc causes irreversible tertiary structural change while the secondary structure remains unchanged. Zinc binding leads to enhanced thermal stability of the LC, which is not identical in the native holo-LC and re-Zn^{2+}-LC.

Botulinum neurotoxins (BoNTs,[1] types A−G) are secreted by *Clostridium botulinum* and are responsible for the neuroparalytic syndrome of botulism characterized by flaccid paralysis (*1*). BoNTs are comprised of three domains: a catalytic light chain (LC), a transmembrane N-terminal half of heavy chain (H_N), and a receptor-binding C-terminal half of heavy chain (H_C). The LC and the heavy chain (HC) are linked through a disulfide bond. While the heavy chain facilitates binding of BoNT to the presynaptic membrane and translocation of the LC into the cytoplasm (*2*, *3*), the LC acts as an endopeptidase exclusively on one of the three SNARE (soluble NSF attachment protein receptor) proteins, SNAP-25 (synaptosomal-associated protein of 25 kDa), syntaxin, and VAMP/synaptobrevin (*4*−*9*). The cleavage of SNAP-25 prohibits docking and fusion of synaptic vesicles containing acetylcholine, thus blocking the neurotransmitter release.

In recent years, substantial progress has been made in defining the intracellular biological activity of the neurotoxin by identifying its zinc endopeptidase activity. Its structure (*10*), unique sequence around the zinc-binding motif, site, and specificity of action, in terms of both the target and peptide bond cleaved, identify BoNTs as a new group of zinc endopeptidases (*11*−*13*).

Unique features of the BoNT endopeptidase activity include a deeply (24 Å) buried Zn^{2+}-binding HEXXH motif of the active site (based on X-ray crystallography of BoNT/A; *10*), irreversible loss of biological activity upon removal of bound Zn^{2+} (*11*), activation of the Zn^{2+} endopeptidase activity after reduction of the disulfide bond between the light and heavy chains (*4*, *14*, *15*), activation of the Zn^{2+} endopeptidase activity by a group of neurotoxin-associated proteins (NAPs) (*16*), and dual role (structural as well as functional) of the bound Zn^{2+} in BoNT/A (*14*). To understand the molecular basis of unique features of BoNT endopeptidase activity, it is important to examine the role of Zn^{2+} bound to the active site of BoNT in its endopeptidase activity and polypeptide folding.

Previous study that indicated both the structural and catalytic role of Zn^{2+} endopeptidase activity was carried out with the whole BoNT/A containing both light and heavy chains (*14*). In this report, we present experimental results of the structural and functional role of Zn^{2+} in the recombinant Zn^{2+} endopeptidase subunit (light chain) of BoNT/A. Our results suggest that while the Zn^{2+} binding to the BoNT/A light chain is totally reversible, the latter's endopeptidase activity is reversible only by about 30%. The structural basis of only partial reversibility of the endopeptidase activity appears to lie in the irreversibility of the tertiary structural folding of the BoNT/A light chain.

MATERIALS AND METHODS

Determination of Protein and Zinc Content. For preparation of the apo-LC and removal of contaminating metals,

† This work was supported in part by a grant from the National Institute of Neurological Disorders and Stroke, National Institutes of Health (NS33740). B.R.S. is a Henry Dreyfus Teacher−Scholar.

* Address correspondence to this author at the Department of Chemistry and Biochemistry, University of Massachusetts Dartmouth, 285 Old Westport Road, Dartmouth, MA 02747. Phone: 508-999-8588. Fax: 508-999-8451. E-mail: bsingh@umassd.edu.

[1] Abbreviations: BoNT/A, *Clostridium botulinum* type A neurotoxin; HC, heavy chain of BoNT; LC, light chain of BoNT; SNAP-25, synaptosomal-associated protein of 25 kDa; SNARE, soluble NSF attachment protein receptor; NAPs, neurotoxin associated proteins; EDTA, ethylenediaminetetraacetate; Tris, tris(hydroxymethyl)aminomethane; SDS−PAGE, sodium dodecyl sulfate−polyacrylamide gel electrophoresis; CD, circular dichroism.

10.1021/bi0007472 CCC: $19.00
Published on Web 08/02/2000

the LC was treated with 10 mM ethylenediaminetetraacetate (EDTA) for 1 h at room temperature and dialyzed against metal-free buffer (20 mM Tris, 50 mM NaCl, pH 7.0), as described before (*14*). Total Zn^{2+} concentration was determined with a Perkin-Elmer 5100 (PC, Norwalk, CT) atomic absorption spectrophotometer, as described previously (*17*). All values shown are averages of three independent determinations. The protein concentration was determined spectrophotometrically using a molar extinction coefficient at 280 nm of 0.83 mg^{-1} mL cm^{-1} (*17*).

Circular Dichroism Measurements. Circular dichroism (CD) spectra of the enzyme were acquired with a Jasco J-715 spectrometer. Far-UV CD spectra in the 190−250 nm region were recorded with 1.0 mm path-length cells containing 0.2 mg/mL protein in 20 mM Tris-HCl (pH 7.0) and 50 mM NaCl. Near-UV CD spectra (250−310 nm) were obtained with a 10 mm cell containing 0.8 mg/mL protein in the same buffer. Typically, a scanning rate of 20 nm/min, a response time of 8 s, and a bandwidth of 1.0 nm were used. Spectral resolution was 0.5 nm, and four scans were averaged per spectrum. Final spectra, representing the average of at least five tracings, were corrected for the buffer spectrum. Ellipticities were normalized to residue concentration using the relationship $[\theta] = \theta_{ob}/(lcN)$, where $[\theta]$ is the mean residue ellipticity, θ_{ob} the observed ellipticity, l the path length (in mm), c the molar concentration of the protein, and N the total number of amino acid residues in one protein molecule.

Thermal Denaturation. Thermal denaturation was followed by monitoring the ellipticity at 222 nm. The temperature was increased with a heating rate of 2 °C/min from 25 to 80 °C. Thermal denaturation curves monitored at 280 nm were smoothed using a five-point window to reduce data fluctuation observed due to the low CD signal in the near-UV region.

Fluorescence Lifetime Measurement. Fluorescence lifetime measurements were carried out on an ISS-K2 multifrequency cross-correlation phase and modulation fluorometer (ISS Corp., Champaign, IL) using an excitation wavelength of 295 nm. The cuvette was washed with 20% HNO_3 prior to use. For all of the fluorescence measurements, the temperature of the sample was kept at 10 °C using a water circulating bath (NESLAB, RTE-Series, Portsmouth, NH). Lifetime data were acquired using 12 modulation frequencies, logarithmically spaced from 2 to 200 MHz. Scattered excitation light was removed from the emission beam by a 335 nm high-pass filter. All lifetime measurements were made with the emission polarizer at the magic angle of 54.7° relative to the vertically polarized excitation beam and with *p*-terphenyl in absolute ethanol in the reference cuvette. At each frequency, data were accumulated until the standard deviations of the phase and modulation ratio were below 0.2° and 0.02, respectively, and these values were used as the standard deviation for the measured phases and modulation ratios in all subsequent analysis. The emission decay data were analyzed using the software provided by ISS Inc. The Trp fluorescence lifetime was modeled with two Lorentzian distributions. The fraction was allowed to vary along with the centers of the two Lorentzian distributions, Lor1 and Lor2, and the widths of the distributions at half-height, w_1 and w_2.

Enzymatic Activity and Determination of the Kinetic Parameters. The procedure for the kinetic analysis of SNAP-25 cleavage by the BoNT/A LC was carried out by a method similar to that described by Li et al. (*17*). Briefly, a series of concentrations of SNAP-25 (40, 27, 18, and 12 μM) were incubated at 37 °C with different forms of the LC (holo, apo, and Zn^{2+}-replenished) (20 nM) in 20 mM Tris, pH 7.0, containing 50 mM NaCl for 5 min. The hydrolyzed samples were separated on a SDS−PAGE gel (10%) and stained with Coomassie blue. The reaction was terminated by addition of SDS−PAGE sample buffer.

The hydrolysis of the SNAP-25 was monitored by following the decrease in band intensity on the SDS−PAGE gel determined by analysis of densitometry scans. K_m and k_{cat} values were derived from initial rate measurements as determined as the decrease in SNAP-25 over a 5 min reaction time.

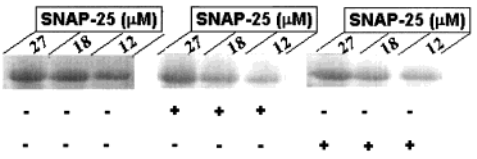

FIGURE 1: Cleavage of SNAP-25 (12, 18, and 27 μM) by 20 nM LC and re-Zn^{2+}-LC.

Table 1: Zinc Content of the Holo-, Apo-, and Re-Zn^{2+}-LC[a]

protein	Zn^{2+} (mol/mol of protein)
holo-LC	1.11 ± 0.21
apo-LC	0.11 ± 0.05
re-Zn^{2+}-LC	1.01 ± 0.22

[a] Data are presented as means ± SD (n = 3). Standards containing zinc ranged from 15.4 to 92.4 nM. Measured values ranged from 18.5 to 65.2 nM.

RESULTS

Reversibility of Zinc Binding. After dialysis against metal-free buffer, the holo-LC contained 1 mol equiv of Zn^{2+}/mol of protein, and the Zn^{2+} content in the apo-LC was negligible (Table 1). When the apo-LC was incubated with 5-fold molar excess of Zn^{2+} and then dialyzed overnight against metal-free buffer, the zinc content was fully restored in the re-Zn^{2+}-LC.

Enzyme Kinetics. SDS−PAGE analysis of the cleavage pattern of SNAP-25 by the holo- and re-Zn^{2+}-LC is shown in Figure 1. Relatively less cleavage of SNAP-25 by the re-Zn^{2+}-LC than the holo-LC is obvious from the relative band intensity of SNAP-25 remaining after the cleavage. However, enzyme kinetic parameters are needed to obtain quantitative comparison of the enzyme activity of the holo- and re-Zn^{2+}-LC. The kinetic parameters were calculated by plotting the initial rate of cleavage as a function of SNAP-25 concentrations. The reaction was found to progress linearly with time within the 5 min observation period. Therefore, the use of a 5 min period for calculating the initial rate of cleavage is appropriate. To establish whether the zinc ion binding to the active site is reversible, the enzymatic activity of the holo- and re-Zn^{2+}-LC was compared. Kinetic constants of different forms of the LC are summarized in Table 2. The Zn^{2+}-depleted LC completely lost the endopeptidase activity. Both the holo- and re-Zn^{2+}-LC were found to be active with k_{cat} values of 140 and 72 min^{-1}, respectively, indicating that zinc replenishment could not fully restore the LC's activity. The

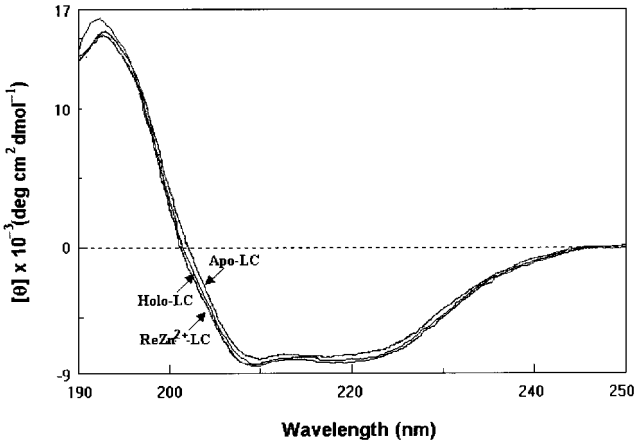

FIGURE 2: Far-UV circular dichroism spectra of the holo-, apo-, and re-Zn^{2+}-LC recorded at 10 °C in 20 mM Tris-HCl (pH 7.0) and 50 mM NaCl. Protein concentrations were 0.2 mg/mL.

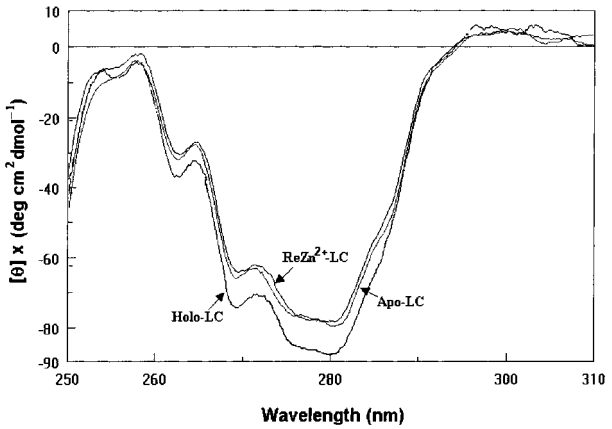

FIGURE 3: Near-UV circular dichroism spectra of the holo-, apo-, and re-Zn^{2+}-LC recorded at 10 °C in 20 mM Tris-HCl (pH 7.0) and 50 mM NaCl. Protein concentrations were 1 mg/mL.

Table 2: Enzyme Kinetic Parameters for the Holo-, Apo-, and Re-Zn^{2+}-LC[a]

enzyme	K_m (μM)	k_{cat} (min^{-1})	k_{cat}/K_m (μM^{-1} min^{-1})
holo-LC	41 ± 10	140 ± 51	3.2
apo-LC		nd[b]	nd
re-Zn^{2+}-LC	55 ± 19	72 ± 21	1.1

[a] Data are presented as means ± SD (n = 3). [b]nd: not detectable.

Table 3: Tryptophan Lifetimes in the Holo-, Apo-, and Re-Zn^{2+}-LC[a]

	f_1	τ_1 (ns)	f_2	τ_2 (ns)	χ^2
holo-LC	0.90	2.08 ± 0.11	0.10	0.60 ± 0.10	5.5
apo-LC	0.86	2.70 ± 0.10	0.14	0.69 ± 0.13	4.5
re-Zn^{2+}-LC	0.87	2.58 ± 0.12	0.13	0.65 ± 0.10	5.6

[a] All measurements were carried out in triplicate, and mean data are presented along with the standard deviation (n = 3). Excitation wavelength = 295 nm.

K_m values are similar for the holo- and re-Zn^{2+}-LC, 41 and 55 μM, respectively, especially in view of the over 30% range in the standard deviation in the experimental data (Table 2). The k_{cat}/K_m values showed a 3-fold difference in the catalytic efficiency of the holo- and re-Zn^{2+} BoNT/A LC.

Structural Analysis of the Holo-, Apo-, and Re-Zn^{2+}-LC. The secondary structure of globular proteins is readily probed by far-UV CD measurements. The far-UV CD spectra of the holo-, apo-, and re-Zn^{2+}-LC are presented in Figure 2. The far-UV CD spectra corresponding to the three LC forms are dominated by strong CD bands at 208 and 222 nm, indicating their highly helical nature. The far-UV CD spectrum of the Zn^{2+}-bound LC is almost indistinguishable from that of the metal-free LC. The secondary structure did not appear to undergo any major change, indicating that the main peptide backbone folding is not significantly altered by the removal of Zn^{2+}.

The near-UV CD technique helps to probe protein tertiary structural changes that affect the environment of aromatic side chains. The near-UV CD spectra of the three forms of the LC are dominated by a major negative band at 280 nm (Figure 3), corresponding to asymmetry around Tyr residues. In addition, there is a negative near-UV CD band with a maximum amplitude at 270 nm, which is attributed to the Phe residues. The shoulder at 286 nm can be attributed to the two Trp residues (*17*). The intensity of near-UV CD signal decreased significantly (10%) when zinc was removed. The decrease in the CD signal of the apo-LC was observed at both 270 and 280 nm, indicating perturbations in the environment of Phe and Tyr, respectively. Replenishment of the apo-LC with Zn^{2+} did not cause any change in its near-UV CD spectrum, indicating irreversibility of structural change induced by the removal of Zn^{2+} of the BoNT/A LC. The intensities of the two negative peaks at 270 and 280 nm were distinctly lower in the apo- and re-Zn^{2+}-LC, suggesting a looser hydrophobic core containing Phe and Tyr residues. It seems that removal of the zinc induces irreversible conformational changes in the protein tertiary structure. The near-UV CD spectrum reflects changes in the asymmetry of the environment, and these are much less pronounced at 286−292 nm (Trp residues) than at 255−270 (Phe) and 275−282 nm (Tyr).

The two tryptophan residues in the holo-LC are predicted to be located in a hydrophobic core (*17*); we used these intrinsic fluorophores as reporters of local environmental changes which arise from removal of zinc in tryptophan fluorescence lifetime studies (Table 3). The longer lifetime component (τ_1) increased from 2.08 to 2.70 ns when zinc is removed. Replenishment of Zn^{2+} shifted τ_1 to a value of 2.58 ns. The shorter lifetime component (τ_2) remained unchanged in all three forms of the LC.

When the analysis was carried out in terms of a distribution of lifetimes, a significant change in the lifetime heterogeneity was observed. The recovered lifetime distributions obtained from the analysis of the data are plotted in Figure 4. The increase in the heterogeneity of emission in the re-Zn^{2+}-LC is evidenced by the increase in the width of the distribution compared to the holo- and apo-LC.

Temperature-Induced Conformational Transitions. The thermally induced denaturations of the secondary and tertiary structures of the LCs were monitored by following the loss of ellipticity of the CD band at 222 and 280 nm, respectively (Figures 5 and 6). Temperature-dependent CD signals in both the far- and near-UV regions showed typical S-shaped denaturation curves. Although the thermal denaturation was irreversible, precluding the determination of thermodynamic parameters, the transition curves based on both far-UV and

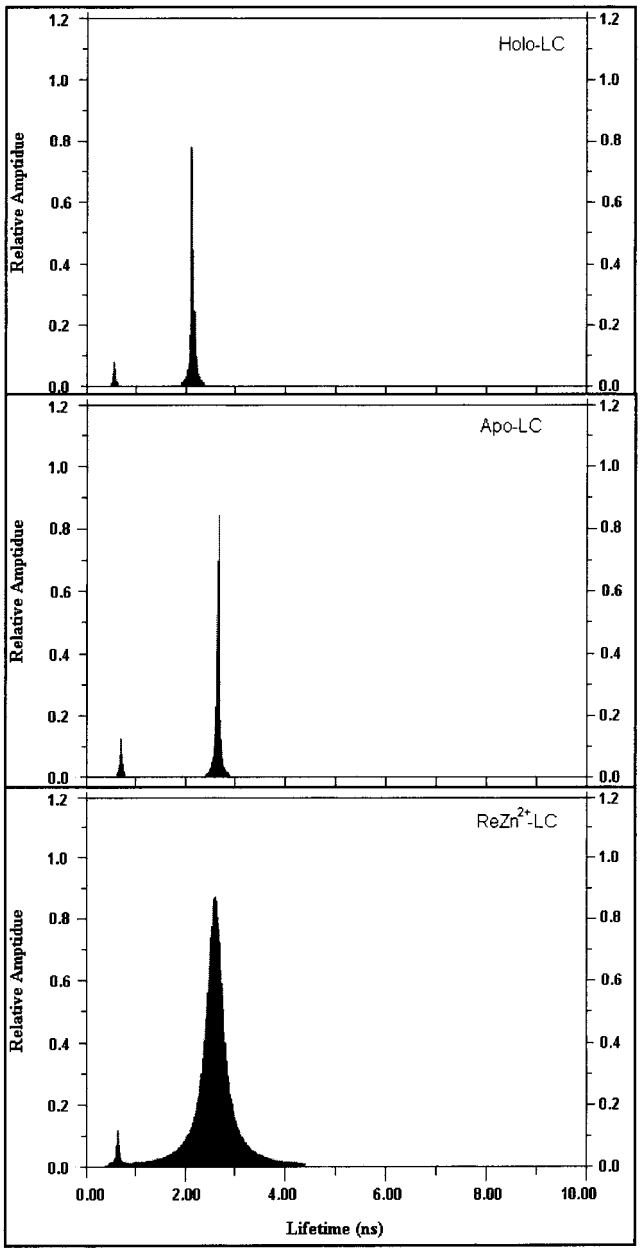

FIGURE 4: Tryptophan fluorescence lifetime distribution profiles obtained from analysis of the data in Table 3. As the protein undergoes conformational change upon removal and replenishment of Zn^{2+}, the peak center shifts to higher lifetime values. The increase in the lifetime heterogeneity of the re-Zn^{2+}-LC is evidenced by the increase in the width of the distribution.

near-UV CD signals indicated apparent T_m values of 52, 44, and 52 °C for the holo-, apo-, and re-Zn^{2+} BoNT/A LC, respectively (Figures 5 and 6). The lower T_m value observed for the apo-LC indicates that the apo-LC is less heat stable than the holo- and re-Zn^{2+} forms. The holo-LC exhibits a gradual and continuous decrease in ellipticity (corresponding to the loss of secondary structure) between 42 and 60 °C rather than an abrupt, cooperative pattern of unfolding. For the apo-LC, denaturation occurs with a sharp transition of the native protein to the denatured form (i.e., from an ellipticity of −25 mdeg to one of −5 mdeg) between 40 and 48 °C (Figure 5). For the re-Zn^{2+}-LC, there is a gradient (change in ellipticity per degree Celsius) similar to that of the apo-LC but with higher T_m, similar to the holo-LC. The sharp cooperative transition from the initial folded to the final

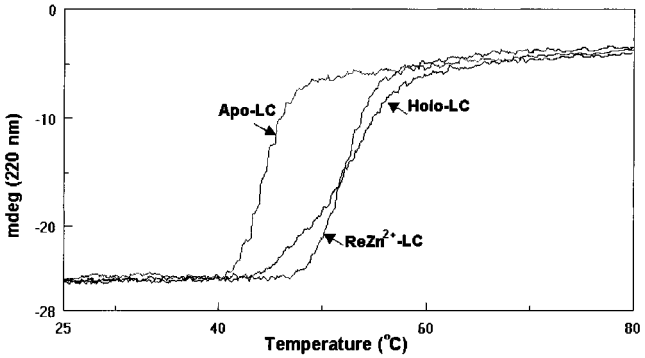

FIGURE 5: Thermal denaturation of the holo-, apo-, and re-Zn^{2+}-LC at the secondary structure level as monitored at 220 nm.

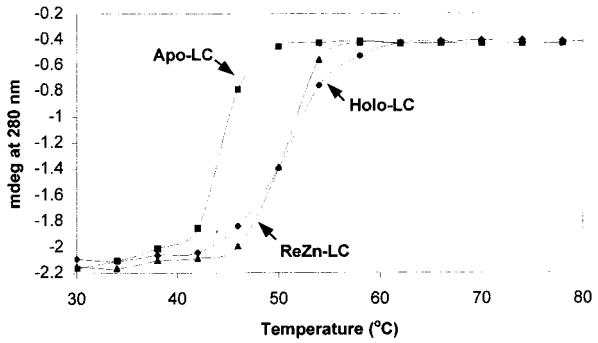

FIGURE 6: Thermal denaturation of the holo-, apo-, and re-Zn^{2+}-LC at the tertiary structure level as monitored at 280 nm. The transition curves were recorded at a resolution of 0.1 °C and were smoothed for clarity in the presentation.

unfolded state indicates that intermediate states are energetically unfavorable and not stabilized. An interesting point worth reemphasizing is the identical denaturation curves and T_m values observed for the holo-, apo-, and re-Zn^{2+}-LC in both far-UV and near-UV CD analysis.

DISCUSSION

The LC was selected for a thorough study in this work by a combination of CD and fluorescence spectroscopy because of its catalytic significance and intriguing structural properties. Recent structural data of BoNT/A revealed significant differences in Zn^{2+}-induced conformational changes (*14*). On the basis of these results and the known zinc endopeptidase activity, zinc binding is believed to have both structural and functional roles in the toxin. In this report, we aimed to investigate the Zn^{2+}-binding characteristics of the enzymatic subunit of BoNT/A, the LC, and structural properties that are related to the Zn^{2+}-binding status.

In general, zinc is known to constitute an integral part of a large number of enzymes involved in virtually all aspects of metabolism (*18*). On the basis of the X-ray analysis of a variety of zinc enzymes, three major zinc-binding motifs exist, i.e., catalytic, cocatalytic, and structural (*19*). Here we demonstrate that the zinc ion can be removed from its binding site in the BoNT/A LC by the chelating agent EDTA. This made it possible to compare the holo- and apo-LC in order to investigate the possible function of the Zn^{2+} in the LC.

Although far-UV CD experiments revealed no change in secondary structure upon removal of Zn^{2+} (Figure 2), evidence for Zn^{2+}-induced conformational changes of the apo-LC came from near-UV CD and fluorescence spectro-

photometric experiments (Figures 3 and 4). The irreversible decrease in signal in the near-UV CD region by removal of Zn^{2+} reveals that the tertiary structure is perturbed by Zn^{2+} removal, which cannot be restored by Zn^{2+} replenishment. This understanding was further supported by Trp fluorescence lifetime data (Table 3). Compared to the holo-LC, a higher Trp fluorescence lifetime value was observed for the two other forms of the LC, indicating dequenching of Trp fluorescence by amino acid side chains. This observation is consistent with the removal of quenching effect by other residues in a less folded structure (*17*). The above data suggest that the apo- and re-Zn^{2+}-LC showed rearrangements in the environment of the aromatic residues with less rigid structure. Our recent study has shown that the Trp residues are constrained in a hydrophobic protein core, with quenched fluorescence lifetime by nearby residues in the folded state (*17*). Upon denaturation of the protein by urea, both τ values shift to longer lifetime. It is reasonable to conclude that removal of zinc creates a less quenching environment in the vicinity of the τ_1 corresponding residue Trp-118 (*17*), resulting in an increased fluorescence lifetime value. On the other hand, the unchanged τ_2 value suggests the microenvironment surrounding Trp-43 is not sensitive to zinc depletion. A wider range of lifetime distribution was observed for the re-Zn^{2+}-LC (Figure 4), indicating that the re-Zn^{2+}-LC experiences increased structural flexibility at least in the vicinity of Trp residues, which is different from structural characteristics of both the holo- and apo-LC. While Zn^{2+} replenishment did not result in the restoration of the Trp fluorescence lifetime, the broad distribution represents perhaps a partial restoration of the active structure. This slight recovery of structural characteristics is concomitant with the partially restored endopeptidase activity in the re-Zn^{2+}-LC. The structural heterogeneity of the re-Zn^{2+}-LC could arise in two ways: (1) Differential location of bound Zn^{2+}. Zn^{2+} binds to a position other than the active site in a significant fraction of the apo-LC molecules, resulting in the total loss of endopeptidase activity in these re-Zn^{2+}-LC molecules. (2) Perturbation of the metal coordination sphere. Zn^{2+} binds to the same active site with a different coordination to the ligands, or with fluctuating zinc binding site structure, which leads to less than optimal activity of the re-Zn^{2+}-LC. Coordination ligands of Zn^{2+} in the BoNT/A LC are known to involve His-223, Glu-224, His-227, and Glu-262, as well as Tyr-366 (*10*). The involvement of distal residues in Zn^{2+} binding points to its structural role beyond the active site. In a previous study (*17*), we have shown that specific coordination and geometry are required in the active site for an optimal endopeptidase activity of the BoNT/A LC. Since the zinc content in the re-Zn^{2+}-LC is optimally restored, the possibility of zinc binding to other sites is less likely. In other words, if there were more than one Zn^{2+}-binding site, one would expect more than 1 to 1 stoichiometry between Zn^{2+} and the BoNT/A LC. On the basis of these observations, we believe that the heterogeneity in the structure of the re-Zn^{2+}-LC originates from the heterogeneity in the Zn^{2+} binding to the active site, perhaps due to a fluctuating polypeptide folding, which also manifests its effect on Trp fluorescence.

Temperature denaturation T_m was significantly decreased from 52 to 44 °C upon removal of Zn^{2+}. The strong point of the thermal resistance of the holo-LC is the tightening of the structural zinc and thus of the catalytic core where the metal is complexed by the His-223, Glu-224, His-227, Glu-262, and Tyr-366 residues (*10*). Decreased near-UV CD signal and increased Trp fluorescence lifetime in the apo-LC suggest that the protein experiences increased structural flexibility and loses its tight packing upon Zn^{2+} depletion. As far as the influence of zinc on thermal stability of the BoNT/A LC global structure is concerned, we hypothesize that long-range effects are involved, presumably across hydrogen bond networks or electrostatically through space within the protein scaffolding. To function optimally, the LC maintains a proper balance of rigidity and flexibility. Zinc binding shifts this balance slightly toward the former, resulting in greater thermal resistance in the holo- and re-Zn^{2+}-LC.

The temperature denaturation profile of the holo-LC has revealed some peculiarities: the unfolding transitions occur over a significantly broader temperature range than those of the apo- and re-Zn^{2+} (Figures 5 and 6), suggesting that the holo-LC unfolding is less cooperative. This is unexpected for a metal-binding protein where more cooperative folding is provided by the metal (*20*). The way to account for these data is to assume that the unfolding transition of the holo-LC is not accurately described by a two-state model. It is possible that the broad peak results from two unresolved transitions with one of them corresponding to distortion of the zinc-binding site. In comparison to the re-Zn^{2+}-LC, the start of the holo-LC thermal denaturation is clearly at lower temperature, indicating a less stable structure for the first transition, while the end of denaturation is at higher termperature, corresponding to a more stable structure for the last transition. We therefore presume that both a flexible and rigid structure is present in the holo-LC, which unfolds at different temperatures. It is plausible to consider that replenishment of Zn^{2+} in the apo-LC is accompanied by repositioning of toxic segments in the protein, resulting in a loosely packed structure. This delocalized binding of Zn^{2+} to the active site might be the reason that the re-Zn^{2+}-LC behaves differently from the holo-LC during temperature denaturation. The cooperative unfolding of the re-Zn^{2+}-LC is consistent with an all-or-none transition of the unfolded state (*21*) observed in less rigid protein structures, such as molten globule protein.

Examination of the endopeptidase activity of the holo-, apo-, and re-Zn^{2+}-LC highlights two important features, namely, the reversibility of the zinc endopeptidase activity and the high susceptibility of SNAP-25 to different LCs. Although the specific activity was different in the holo- and re-Zn^{2+}-LC, the binding affinity to the substrate was similar, K_m of 41 and 55 μM, respectively. It is therefore likely that the tighter tertiary structure in the holo form may not be important for its interaction with the target protein. Thus we can conclude that the presence of only partial enzymatic activity in the re-Zn^{2+}-LC is largely due to the impaired k_{cat} only. In the holo form, the LC rapidly cleaved SNAP-25, suggesting that the residues in the scissile bond of the substrate are in close proximity of Zn^{2+}. In the re-Zn^{2+}-LC form, the LC may undergo a conformational change upon replenishing with Zn^{2+}, leading to a partially active enzyme. It could be speculated that the apo-LC binds Zn^{2+} to give an incorrectly folded form in which certain active site residues are not optimally coordinated to the zinc in the re-

Zn^{2+}-LC. Alternatively, the slow endopeptidase activity of the re-Zn^{2+}-LC could be due to the shielding of active site residues due to a rearrangement of neighboring amino acids.

Due to the irreversibility of the structural and functional change introduced by zinc removal, the question remains as to what controls the zinc-binding event for optimal activity of the enzyme during protein synthesis of the LC in vivo. Other protein interactions with the LC could conceivably alter its conformation in ways that might facilitate the correct folding of the LC. In this context it is important to note that the biological activity of BoNT/A, containing both the LC and HC, was totally lost upon removal of Zn^{2+} (*14*), and not even the partial restoration was achieved with Zn^{2+} replenishment. The presence of the HC therefore makes the LC's active structure more labile to irreversible change.

In summary, we have demonstrated that Zn^{2+} binding provides structural stability in the LC in addition to its catalytic role. Binding of the zinc to the protein is reversible while the tertiary structural change upon zinc removal is irreversible. The enzymatic activity of the LC was recovered by only about one-third upon Zn^{2+} replenishment.

REFERENCES

1. Poulain, B. (1994) *Pathol. Biol. (Paris) 42*, 173−182.
2. Lebeda, F. J., and Singh, B. R. (1999) *Toxin Rev. 18*, 45−76.
3. Ahnert-Hilger, G., and Bigalke, H. (1995) *Prog. Neurobiol. 46*, 83−96.
4. Blasi, J., Chapman, E. R., Link, E., Binz, T., Yamasaki, S., De Camilli, P., Sudhof, T. C., Niemann, H., and Jahn, R. (1993) *Nature 365*, 160−163.
5. Blasi, J., Chapman, E. R., Yamasaki, S., Binz, T., Niemann, H., and Jahn, R. (1993) *EMBO J. 12*, 4821−4828.
6. Yamasaki, S., Hu, Y., Binz, T., Kalkuhl, A., Kurazono, H., Tamura, T., Jahn, R., Kandel, E., and Niemann, H. (1994) *Proc. Natl. Acad. Sci. U.S.A. 91*, 4688−4692.
7. Yamasaki, S., Binz, T., Hayashi, T., Szabo, E., Yamasaki, N., Eklund, M., Jahn, R., and Niemann, H. (1994) *Biochem. Biophys. Res. Commun. 200*, 829−835.
8. Foran, P., Shone, C. C., and Dolly, J. O. (1994) *Biochemistry 33*, 15365−15374.
9. Li, L., and Singh, B. R. (1999) *J. Nat. Toxins−Toxin Rev. 18*, 95−112.
10. Lacy, D. B., Tepp, W., Cohen, A. C., DasGupta, B. R., and Stevens, R. (1998) *Nat. Struct. Biol. 5*, 898−902.
11. Montecucco, C., and Schiavo, G. (1993) *Trends Biochem. Sci. 18*, 324−327.
12. Tonello, F., Morante, S., Rossetto, O., Schiavo, G., and Montecucco, C. (1996) *Adv. Exp. Med. Biol. 389*, 251−260.
13. Pellizzari, R., Rossetto, O., Schiavo, G., and Montecucco, C. (1999) *Philos. Trans. R. Soc. London, Ser. B 354*, 259−268.
14. Fu, F. N., Lomneth, R. B., Cai, S., and Singh, B. R. (1998) *Biochemistry 37*, 5267−5278.
15. Schiavo, G., Benfenati, F., Poulain, B., Rossetto, O., Polverino de Laureto, P., DasGupta, B. R., and Montecucco, C. (1992) *Nature 359*, 832−835.
16. Cai, S., Sarkar, H. K., and Singh, B. R. (1999) *Biochemistry 38*, 6903−6910.
17. Li, L., and Singh, B. R. (2000) *Biochemistry 39*, 6466−6474.
18. Lipscoomb, W. N., and Strater, N. (1996) *Chem. Rev. 96*, 2375−2433.
19. Vallee, B. L., and Auld, D. S. (1990) *Proc. Natl. Acad. Sci. U.S.A. 87*, 220−224.
20. Arnold, F. H., and Zhang, J. H. (1994) *Trends Biotechnol. 12*, 189−192.
21. Ptitsyn, O. B. (1995) *Curr. Opin. Struct. Biol. 5*, 74−78.

BI0007472